Ferromagnetic states in the $In_{1-x}Mn_xSe$ layered crystal

V. V. Slyn'ko,[1] A. G. Khandozhko,[1] Z. D. Kovalyuk,[1] V. E. Slyn'ko,[1] A. V. Zaslonkin,[1] M. Arciszewska,[2] and W. Dobrowolski[2]

[1]*Institute for Problems of Materials Science, NASU, Vilde 5, 58001 Chernovtsy, Ukraine*

[2]*Institute of Physics, Polish Academy of Sciences, Al.Lotników 32/46, 02-668 Warsaw, Poland*

(Received 2 November 2004; revised manuscript received 3 March 2005; published 3 June 2005)

Electron paramagnetic resonance, magnetization, and dynamic magnetic susceptibility have been investigated in the new member of the semimagnetic semiconductors family, $In_{1-x}Mn_xSe$ layered crystal with composition $x=0.0125$. The obtained results indicate that two subsystems of impurity manganese ions exist in the examined crystal: the first one inside the crystal layer and the second one in the interlayer space. It is found that at low temperatures, below 77 K, three-dimensional ferromagnetic order arises in the as-grown sample. In the annealed sample, two-dimensional ferromagnetism is observed in the interlayer space.

DOI: 10.1103/PhysRevB.71.245301 PACS number(s): 75.30.Hx, 75.70.Cn, 75.20.Ck

I. INTRODUCTION

A common feature of layered III-VI semimagnetic semiconductors (SMSC) is their quasi-two-dimensional crystal structure. The crystals are comprised of four-atom thick two-dimensional layers: a top anion layer, two middle cation layers, and a bottom anion layer. Those four-atom thick layers are bonded with the weak van der Waals interaction, while inside them bonds are covalent. The same as in the II-VI SMSC, substitutional magnetic ions in the layered III-VI SMSC are in a tetrahedral environment. However, due to the crystal structure in the III-VI mixed crystals, each magnetic ion has only three neighboring anions and the fourth nearest neighbor is another cation, either a magnetic or nonmagnetic one. As a result, more complicated exchange channels may be realized in the layered III-VI SMSC than in the case of II-VI SMSC (see, e.g., Fig. 1 in Ref. 1).

In this respect Refs. 1 and 2 are of interest, in which the temperature and field dependences of magnetization of, respectively, $Ga_{1-x}Mn_xSe$ ($x=0.012$) and $Ga_{1-x}Mn_xS$ ($x=0.011, 0.066$) layered crystals are investigated. It was established that a short-range two-dimensional antiferromagnetic order exists in $Ga_{1-x}Mn_xSe$ in the temperature range 120–195 K. It is supposed that at a temperature of 119 K the transition to three-dimensional order takes place in that crystal as evidenced by a sharp change in magnetization. For the other system, $Ga_{1-x}Mn_xS$, in the temperature range from 75 K to 300 K the magnetization follows the Curie-Weiss law with a negative Curie-Weiss temperature $J_{\mathrm{eff}}/k_{\mathrm{B}}=-50$ K that indicates an antiferromagnetic interaction between the Mn ions.

In view of reported differences in the magnetic behavior of the gallium compounds owing apparently to a change of anion type, it is of interest to study the influence of cation type on the magnetic properties of layered semimagnetic semiconductors. This paper presents measurements of magnetic properties of $In_{1-x}Mn_xSe$ single crystals, namely, electron paramagnetic resonance (EPR), magnetization (M), and dynamic magnetic susceptibility (χ_{ac}).

II. EXPERIMENT

$In_{1-x}Mn_xSe$ single crystals were grown using the Bridgman method at the initial composition of $x=0.01$. Mn distribution along the ingot is nonuniform as determined from energy dispersive x-ray fluorescence analysis (see Fig. 1).

In the initial part of the ingot (up to 0.6 of its length) the Mn content does not exceed a value of 0.15 at. %, while at the end of the ingot Mn concentration values are as high as 3.57 at. %. The samples cut from the ingot had the form of a rectangular plate with typical dimensions of $4\times2\times0.5$ mm^3. The surface of the samples was identical with the cleavage plane (*aa*) perpendicular to the crystal **c** axis.

EPR spectra measurements were carried out at a frequency of 10 GHz using an EPR radiospectrometer with the digital accumulation of a signal. The first derivative of the resonance signal was recorded over the temperature range 77–300 K. The maximum magnetic field reached 5000 Oe. The magnetic field was determined by an NMR probe with an accuracy of ±1 Oe. A DPPH (2,2-diphenyl-1-picrylhydrazyl) reference sample with the total number of spins 5.0×10^{17} and g-factor equal to 2.0036 was used to estimate the spectrometer sensitivity. Separation of the spectrum components was carried out with the help of the specialty computer program for spectral curve decomposition. The line integrated intensity, S, was determined by the numerical double integration of the derivative absorption curve. The peak-to-peak linewidth, ΔH, was defined as the distance

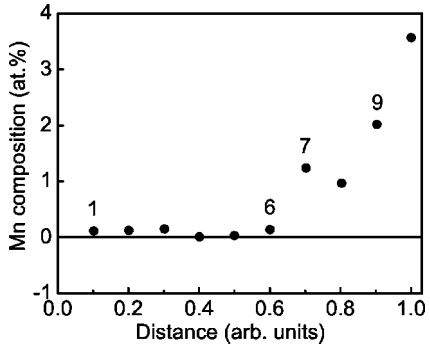

FIG. 1. The Mn distribution along the growth axis of the $In_{1-x}Mn_xSe$ ingot with nominal value $x=0.01$. Labels 1–9 mark the samples described in the text.

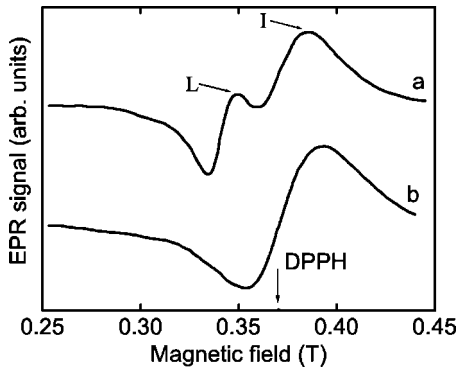

FIG. 2. The EPR spectra of $In_{1-x}Mn_xSe$ samples with $x=0.0125$ at $T=300$ K: a=as grown, b=annealed (for magnetic field **H** oriented at an angle of 55° to the crystal axis **c**). The arrow labeled DPPH corresponds to the reference line with the effective g-factor value 2.0036.

between the minimum and maximum of the first derivative.

Two-function experimental equipment, Lake Shore 7229 AC Susceptometer/DC Magnetometer (with the sensitivity 10^{-7} emu), was used for magnetization and magnetic susceptibility investigations.[3,4] The temperature dependence of dynamic magnetic susceptibility, $\chi_{ac}(T)$, was measured using an ac magnetic field with amplitude of 20 Oe and frequency of 800 Hz over the temperature range 4.2–300 K. Measurements of magnetization $M(H)$ were carried out using magnetizing field $H=40$ Oe for various temperatures (20, 50, and 100 K).

III. RESULTS

At first EPR spectra have been measured on $In_{1-x}Mn_xSe$ as-grown samples cut across to the growth axis of the ingot (Fig. 1). The samples labeled 1–6 with Mn concentrations as low as 0.15 at. % show a very weak EPR signal without any manifestation of a hyperfine structure. The intense resonant absorption is observed for Mn content of the order of 1–2 at. % in the samples 7–9. A two-component EPR spectrum is characteristic of these samples: on a background of a wide line an additional weaker line is registered.

The pronounced two-component EPR spectrum was observed for the as-grown sample 7 with $x=0.0125$ for magnetic field **H** oriented at an angle of 55° to the crystal axis **c**. It consists of two resonant lines, labeled I and L, as shown in Fig. 2 (curve a). The lines are of different widths and reveal different temperature dependences. The further researches of dependences $\Delta H(T)$, $\chi_{ac}(T)$ and $M(H)$ were performed both for the as-grown and annealed samples with $x=0.0125$.

The I linewidth for the as-grown sample is about 370 Oe, and the g-factor is equal to 1.996. Both the parameters do not depend on orientation of magnetic field **H**. At the same time, both in-plane (aa) and out-of-plane (ac) measurements show the strong orientational dependence of the L line at $T=300$ K (Fig. 3, curves 1 and 2, accordingly). The L linewidth changes in the range from about 160 to 200 Oe, and the g-factors at $\mathbf{H}\|\mathbf{c}$ and $\mathbf{H}\perp\mathbf{c}$ are equal to 2.189 and 2.0998, respectively.

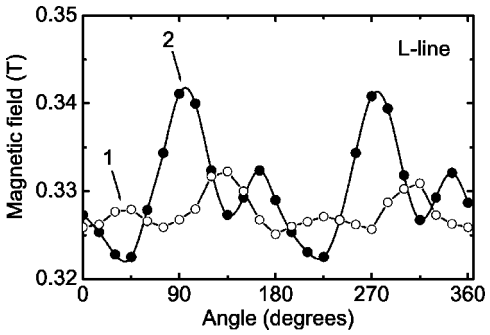

FIG. 3. The angular dependence of the L-resonance position obtained for the as-grown sample at $T=300$ K: 1=in plane (aa), 2=in plane (ac).

An essential difference between the I and L lines is also observed in the temperature dependence of their width, ΔH (see Fig. 4). While the line I broadens monotonically with lowering temperature over the whole interval 300–77 K (curve 1), for the L line the dependence $\Delta H(T)$ is a nonmonotonic one (curve 2). When the temperature decreases from 300 K, the L line narrows and reaches its minimal width at $T\approx 140$ K, then it abruptly broadens as the temperature decreases from 140 to 77 K. The integrated intensities, S_I and S_L, also change nonmonotonically as a function of temperature with maxima at about 140 K (Fig. 5, curves 1 and 3).

Sample annealing in vacuum at $T=593$ K during 28 h substantially changes the EPR spectrum: the L line almost disappears, whereas the I line remains (Fig. 2, curve b). With T decreasing from 300 to 140 K, the I linewidth (Fig. 4, curve 3) and intensity of the I line (Fig. 5, curve 2) grow and, finally, for $T<140$ K, the resonance becomes not visible.

The temperature dependences of both components of dynamic magnetic susceptibility, $\chi_{ac}=\chi_1-i\chi_2$, have complicated character (Fig. 6). For the as-grown sample the real component χ_1 reveals a huge peak at $T=28$ K, and another two, much smaller but distinct, at 190.5 K and 267 K (curve 1). On the temperature dependence of the imaginary component, χ_2, three peaks are also observed: a major one at $T\approx 34$ K, a minor one at 184 K, and a minute peak at 269 K (curve 2).

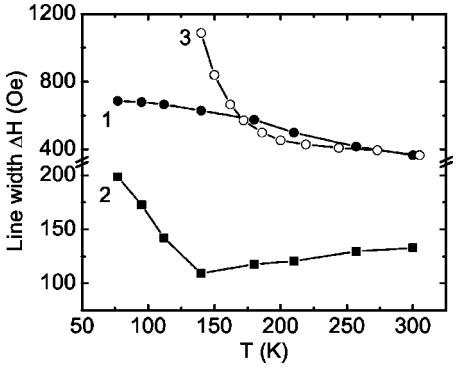

FIG. 4. The temperature dependence of the I and L lines width in $In_{1-x}Mn_xSe$ samples with $x=0.0125$: curves 1 and 2 are the I and L lines for the as-grown sample, accordingly; curve 3 is the I line for the annealed sample.

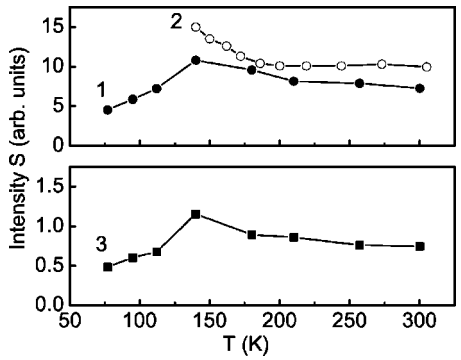

FIG. 5. The temperature dependence of EPR lines integrated intensity for $In_{1-x}Mn_xSe$ ($x=0.0125$): 1 is the I line for the as-grown sample, 2 is the I line for the annealed sample, and 3 is the L line for the as-grown sample.

The *ac* susceptibility of the annealed sample contains only the real component χ_1 (which is in phase with the applied ac field). The character of the dependence of $\chi_1(T)$ did not substantially change after annealing, i.e., the nonmonotonical temperature dependence with three peaks is as before observed (see Fig. 6, curve 3). However, we found that the huge, low-temperature, peak moves into higher temperatures (43 K) as compared to the one observed in the as-grown sample (curve 1).

Rayleigh hysteresis loops were observed at $T=20$ and 50 K in the as-grown sample (Fig. 7).

IV. DISCUSSION

While doping III-VI layered semiconductors two cases are possible: (*i*) impurity atoms may replace host cations in the crystal layer or (*ii*) they may be located in the interlayer space. Of the two, the latter mechanism obviously dominates since to realize it a considerably smaller energy is needed. It is known that an intercalation process in layered crystals (i.e., introducing impurity atoms into the interlayer space) may be realized even at room temperature.[5]

The presence of two lines in the EPR spectrum (Fig. 2, curve *a*) indicates the existence of two various impurity subsystems in the as-grown crystals. It seems natural to assume that the I resonant line (the one of higher intensity) is connected with those Mn atoms that are located in the interlayer space while the L line is connected with the Mn atoms substituting indium atoms inside the crystal layer. An influence of sample annealing on the EPR spectra may be fully understood in consistence with the proposed model. During the annealing process, the Mn ions diffuse from their lattice position into the interlayer space. As a result, the L resonance almost disappears (Fig. 2, curve *b*) and, at the same time, the intensity of the I line increases (Fig. 5, curve 2).

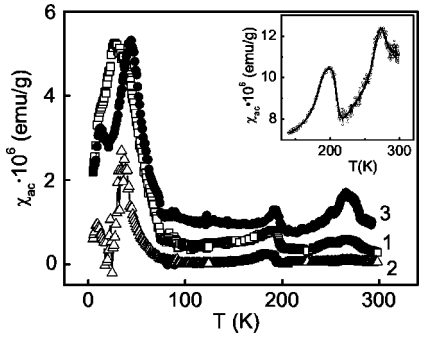

FIG. 6. The temperature dependence of χ_{ac} dynamic magnetic susceptibility for $In_{1-x}Mn_xSe$ ($x=0.0125$): 1 and 2 are the real and imaginary components for the as-grown sample, respectively; 3 is the real component for the annealed sample. The inset shows real component of χ_{ac} vs. T for the as-grown sample with $x=0.037$.

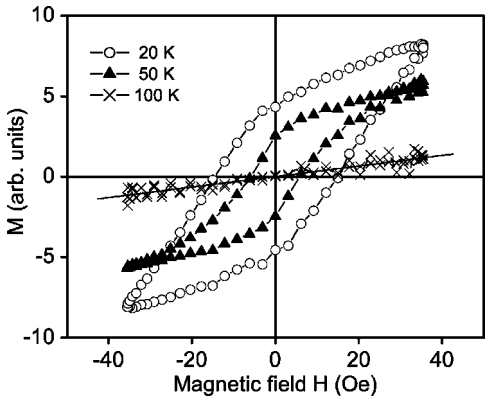

FIG. 7. The Rayleigh hysteresis loops at different temperatures for $In_{1-x}Mn_xSe$ with $x=0.0125$.

The observed directional dependences of the L line and the lack of such dependence for the I line shows that the local fields acting on the Mn ion in the crystal layer and in the interlayer space have different symmetries.

In a crystal, the g-factor depends on the orientation of an external magnetic field relative to the axes of intracrystalline field symmetry.[6] The symmetry of the last one depends on a local arrangement of the nearest diamagnetic ions. The g-factor is a tensor; the number of its components indicates the symmetry of the local field in a crystal. The symmetry is axial if two components are observed, $g_\parallel$ and $g_\perp$ (along the crystal axis **c** and perpendicularly to it) and in plane (*aa*) spectrum has axial symmetry. Hence, the presence of the angular dependence of the L resonance in both crystal planes (*ac*) and (*aa*) indicates that the symmetry of a local field in the crystal layer is lower than axial. To conclude, the lack of angular dependence in the I line case may be explained by the cubic symmetry of a local field in the $In_{1-x}Mn_xSe$ interlayer space.

The observation of the broadened I and L lines evidences by itself that numerous groups of magnetic ions are coupled by exchange interaction.[7,8] The EPR spectrum of isolated Mn^{2+} ions (nuclear spin $I=5/2$) has a hyperfine structure consisting of six lines. Clusters of interacting Mn ions show a hyperfine spectrum with a number of lines directly proportional and a distance between them inversely proportional to the cluster size. At a small number of interacting Mn ions (where Mn singles and pairs dominate) an absorption curve can still have some structure, but for Mn concentrations large enough (larger clusters present) the hyperfine structure disappears and the wide curve of absorption is observed.

The character of temperature dependences of the linewidths, $\Delta H_I(T)$ and $\Delta H_L(T)$, and integrated intensities, $S_I(T)$

and $S_L(T)$, is determined mainly by the type of exchange pairs existing in the interlayer space and inside the crystal layer. In the interlayer space, where the Mn ions are located in slightly distorted tetrahedral hollows formed by the adjacent selenium monolayers,[9] the indirect exchange is possible only via Se ions (Mn-Se-Mn). In the crystal layer, apart from the superexchange in the Mn-Se-Mn pairs (and presumably in Mn-In-Se-Mn pairs), a direct exchange in the Mn-Mn pairs is also possible (see, e.g., Fig. 1 in Ref. 1).

The abrupt decrease of the S_I and S_L (Fig. 5) at simultaneous broadening of the I and L lines with T decreasing from 140 to 77 K (Fig. 4) most probably results from an antiferromagnetic superexchange in the pairs Mn-Se-Mn (and, probably, also in the Mn-In-Se-Mn pairs—in the layer). In turn, the increase of S_I and S_L as temperature decreases from 300 to 140 K indicates the ferromagnetic character of exchange interaction between the Mn ions both in the layer and in the interlayer space.

The observed narrowing of the L line in the range 300–140 K (Fig. 4, curve 2), contrary to the broadening of the I line (curve 1), can be explained by the direct exchange in the nearest-neigbor Mn-Mn pairs, which are present only within the crystal layer. The very fast direct exchange in the Mn-Mn pairs results in averaging of the local fields, acting on a paramagnetic ion, thus leading to the narrowing of the L line.[10]

In Ref. 2 it is supposed that in $Ga_{1-x}Mn_xS$ at $T=10.9$ K a magnetic phase transition to a spin glass state (or cluster locking) may take place that is an unusual phenomenon in quasi-two-dimensional structures. We believe that in the layered crystals ($Ga_{1-x}Mn_xS$ as well as $In_{1-x}Mn_xSe$), at low temperatures, Mn-S/Se-Mn pairs can also be formed with one of the Mn ions located in the interlayer space and the other located inside the crystal layer. The indirect exchange interaction with the participation of such pairs connects neighboring crystal layers and as a consequence the three-dimensional magnetic order occurs.

The character of $\chi_{ac}(T)$ dependence (Fig. 6) as well as the existence of Rayleigh magnetic hysterese (Fig. 7) are direct evidence that a three-dimensional ferromagnetic order exists in some ranges of the as-grown sample (impurity ions clusters) in the range $T<77$ K. The Rayleigh hysteresis loop is an effect of the irreversible process of magnetization in a weak magnetic field (as well as in a case of usual hysteresis). In this case the field dependence of magnetization M for the initial part of the magnetization curve is expressed by the Rayleigh formula:[10,11]

$$M = \chi_a H \pm bH^2, \tag{1}$$

where χ_a is the initial magnetic susceptibility, b is Rayleigh's constant, and the sign + or − corresponds to the magnetic field direction. The constant b is connected with the residual magnetization M_R and saturation field H_m of a hysteresis curve by the relation[10]

$$b = \frac{2M_R}{H_m^2}. \tag{2}$$

Using experimental values of M_R and H_m (Fig. 7) one is able to find the hysteresis loss for the Rayleigh loop:[10]

$$W_h = \frac{1}{4\pi}\oint HdM = \frac{bH_m^3}{3\pi} = \frac{2M_R H_m}{3\pi}. \tag{3}$$

The observed increase of the M_R and H_m values with reduction of temperature in the $In_{1-x}Mn_xSe$ as-grown sample (Fig. 7) corresponds to the increase of hysteresis loss, which is characteristic of typical ferromagnets.

An appearance of imaginary component, χ_2, in the as-grown sample is also caused with the hysteresis loss as a result of irreversible displacement of domain walls since the measurements of $\chi_{ac}(T)$ were carried out at low frequency field.[11] It follows that the absence of an imaginary component, χ_2, in the annealed samples testifies to the absence of domain structure in two-dimensional ferromagnetic clusters, formed in the interlayer space of investigated crystals. It will be noted that eddy-current loss can be neglected because of low concentration of free carriers in $In_{1-x}Mn_xSe$, which at $T=77$ K is below 10^{13} cm^{-3}.

In order to find out what is the possible origin of the high temperature *ac* susceptibility peaks, we shall analyze first the dependencies $\chi_{ac}(T)$ and $S(T)$ for the as-grown sample in distinct temperature intervals. As one can see, two small peaks are observed in the range 300–140 K (Fig. 6), where, according to EPR data (Fig. 5), exchange interaction has ferromagnetic character both in the layer and in the interlayer space. At the same time, in the interval 140–77 K, where antiferromagnetic superexchange occurs, peaks are not observed. Therefore, we suppose that those peaks may be caused only by an existence of a very weak ferromagnetism in the impurity ions clusters. The observed increase of the high-temperature χ_{ac} peaks amplitude with Mn content increasing ($x=0.037$) confirms this hypothesis (see the inset in Fig. 6). The magnetic susceptibility χ_{ac} is overall characteristic of a crystal and thus takes into account the total exposure of all the exchange Mn pairs, existing in the as-grown sample.

The above considerations may be applied, in some measure, to the annealed sample. The distinction is only that all observed peaks on the dependence of $\chi_1(T)$ are due to a formation of the ferromagnetic clusters in the interlayer space, i.e., two-dimensional ferromagnetism arises. During the annealing process, in fact, all the Mn ions diffuse from the crystal layer into the interlayer space. The increase of the Mn ion's quantity in the interlayer space reduces the number of breaks in a chain of interacting Mn ions and, as a consequence, the Curie temperature increases to 43 K (Fig. 6, curve 3) as compared with 28 K found for the as-grown sample (Fig. 6, curve 1). As well as in the as-grown sample, the high temperature peaks are observed in the interval 300–140 K (Fig. 6, curve 3) where ferromagnetic exchange interaction is active (Fig. 5, curve 2).

V. CONCLUSIONS

The results of EPR investigation indicate the existence of two separate quasi-two-dimensional magnetic impurity sub-

systems in the $In_{1-x}Mn_xSe$ ($x=0.0125$) as-grown crystals: the first one is inside the crystal layer and the second one is in the interlayer space. In the temperature range from 300 to 140 K ferromagnetic exchange interaction takes place both in a layer and in an interlayer space. In contrast, antiferromagnetic superexchange happens over the range 140–77 K. At the lowest temperatures (below 77 K), the three-dimensional ferromagnetic ordering of Mn ions appears in the as-grown sample as evidenced by the observation of Rayleigh hysteresis loops and by the character of temperature dependence of dynamic magnetic susceptibility. In the annealed sample two-dimensional ferromagnetism is observed in the interlayer space.

ACKNOWLEDGMENT

This work is partially supported by Science-Technology Center in Ukraine (Project No. NN 36).

[1] T. M. Pekarek, B. C. Crooker, I. Miotkowski, and A. K. Ramdas, J. Appl. Phys. **83**, 6557 (1998).
[2] T. M. Pekarek, M. Duffy, J. Garner, B. C. Crooker, I. Miotkowski, and A. K. Ramdas, J. Appl. Phys. **87**, 6448 (2000).
[3] J. K. Krause and J. R. Bergen, Superconductor Industry **3**, 23 (1990).
[4] F. Gömöry, Rev. Sci. Instrum. **62**, 2019 (1991).
[5] I. I. Grygorchak, Z. D. Kovalyuk, and S. P. Yurtsenyuk, Izv. Akad. Nauk SSSR, Neorg. Mater. **17**, 412 (1981).
[6] W. Low, *Paramagnetic Resonance in Solid* (Academic Press, New York, 1960).
[7] A. Abragam and B. Bleaney, *Electron Paramagnetic Resonance of Transition Ions* (Clarendon Press, Oxford, 1970).
[8] *Hyperfine Interactions*, edited by A. J. Freeman and R. B. Frankel (Academic Press, New York, 1967).
[9] J. C. J. M. Terhell, Prog. Cryst. Growth Charact. **7**, 55 (1983).
[10] S. V. Vonsovskiy, *Magnetizm* (Nauka, Moskwa, 1971).
[11] S. Chikazumi, *Physics of Ferromagnetism* (Oxford University Press, Oxford, 1997).